Dalton Transactions

Accepted Manuscript

This article can be cited before page numbers have been issued, to do this please use: Y. Ma, S. Zhang, H. Wei, Y. Dong, L. Shen, S. Liu, Q. Zhao, L. Liu and W. (. Wong, *Dalton Trans.*, 2018, DOI: 10.1039/C8DT00720A.

ROYAL SOCIETY OF CHEMISTRY

rsc.li/dalton

View Article Online
DOI: 10.1039/C8DT00720A

Table of Content

Enhanced singlet oxygen generation of a soft salt through efficient energy transfer between two ionic metal complexes

Yun Ma, Shujun Zhang, Huanjie Wei, Yafang Dong, Liang Shen, Shujuan Liu, Qiang Zhao*

Li Liu* and Wai-Yeung Wong*

A novel soft salt based photosensitizer was successfully developed for the application in photodynamic therapy of cancer cells for the first time.

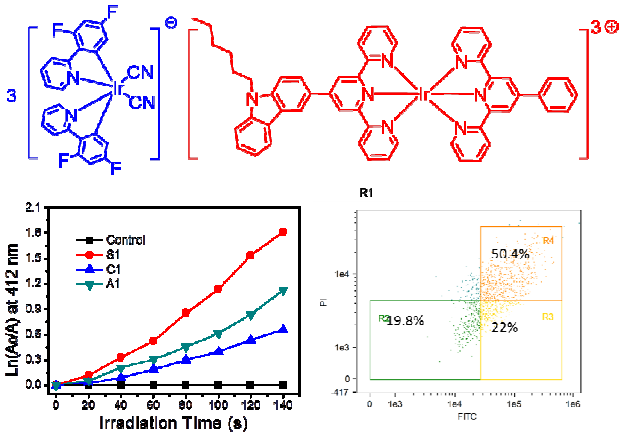

ROYAL SOCIETY OF CHEMISTRY View Article Online
DOI: 10.1039/C8DT00720A

Journal Name

ARTICLE

Enhanced singlet oxygen generation of a soft salt through efficient energy transfer between two ionic metal complexes

Received 00th January 20xx,
Accepted 00th January 20xx

DOI: 10.1039/x0xx00000x

www.rsc.org/

Yun Ma,[ab] Shujun Zhang,[b] Huanjie Wei,[b] Yafang Dong,[b] Liang Shen,[b] Shujuan Liu,[b] Qiang Zhao,[b]* Li Liu,[c]* and Wai-Yeung Wong[ad]*

In this study, a soft salt complex based photosensitizer has been developed for photodynamic therapy (PDT) of cancer cells. The iridium(III) complex $[Ir(L)(L')]^{3+}(PF_6^-)_3$ (**C1**) with L and L' being terpyridine ligands (L = 4'-phenyl-2,2':6',2''-terpyridine, L' = 3-([2,2':6',2''-terpyridin]-4'-yl)-9-hexyl-9H-carbazole) was chosen as the cationic component, and the iridium(III) complex $[Ir(dfppy)_2CN_2]^-Bu_4N^+$ (**A1**) was selected as the anionic component. Complexes **C1** and **A1** are directly connected through electrostatic interaction to form a soft salt based photosensitizer (**S1**), which exhibited enhanced singlet oxygen generation rate because of efficient energy transfer between two ionic metal complexes. Furthermore, this novel photosensitizer was successfully applied in photodynamic therapy (PDT) of cancer cells for the first time.

Introduction

Photodynamic therapy (PDT) is based on the concept that cancer cells are killed by cytotoxic reactive oxygen species (ROS), which is generated from photosensitizers upon light irradiation.[1] As one of the most common toxic ROS, singlet oxygen ($^1O_2$) is generated by energy transfer from the triplet excited state of photosensitizers to the ground state of O_2.[2] Up to now, numerous photosensitizers have been developed for the generation of $^1O_2$, such as organic dyes,[3] conjugated polymers,[4] nanoparticles[5] and transition metal complexes.[6] Among them, transition-metal complexes are most widely used as the photosensitizers due to their high $^1O_2$ generation rate and photostability.[7]

In recent years, a design strategy has been provided for the improvement of the $^1O_2$ generation rate through Förster resonance energy transfer (FRET).[8] However, complex synthesis or modification procedures are required for the preparation of these systems. Especially, the design of transition-metal complex based energy transfer system is still a challenge because of their complicated excited-state properties.[9] Soft salt is composed of an anionic component and a cationic component linked through electrostatic and van der Waals interactions.[10] Recently, soft salts have been successfully applied in organic light-emitting diodes by Thompson and his co-workers.[10a] We have also applied them as phosphorescent ratiometric and lifetime probes for intracellular pH detection.[10b] Nevertheless, much less attention has been paid to the research work of soft salts. The cyclometalated ligands of the two ionic complexes can be easily modified, which are helpful in tuning the absorption and emission peaks of the cationic and anionic components of a soft salt. Therefore, soft salt could be a promising platform for the design of new photosensitizer to enhance $^1O_2$ generation by energy transfer. Until now, however, the use of soft salts in PDT is still an unexplored area.

In the present study, the first example of a soft salt based photosensitizer for the enhancement of $^1O_2$ generation by energy transfer is reported. The iridium(III) complex $[Ir(L)(L')]^{3+}(PF_6^-)_3$ (**C1**) with L and L' being terpyridine ligands

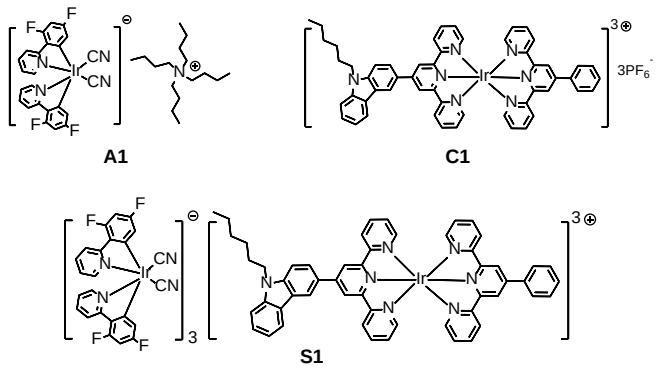

Scheme 1 Chemical structures of complexes **A1**, **C1** and **S1**.

[a] Institute of Molecular Functional Materials and Department of Chemistry, Hong Kong Baptist University, Waterloo Road, Kowloon Tong, Hong Kong, P. R. China. E-mail: rwywong@hkbu.edu.hk
[b] Key Laboratory for Organic Electronics & Information Displays (KLOEID) and Institute of Advanced Materials (IAM), Nanjing University of Posts & Telecommunications (NJUPT), 9 Wenyuan Road, Nanjing 210023, Jiangsu, P. R. China. E-mail: iamqzhao@njupt.edu.cn
[c] Hubei Collaborative Innovation Center for Advanced Organic Chemical Materials, Ministry of Education Key Laboratory for the Synthesis and Application of Organic Functional Molecules, School of Chemistry and Chemical Engineering, Hubei University, Wuhan 430062, Hubei, P. R. China. E-mail: liulihubei@hubu.edu.cn
[d] Department of Applied Biology and Chemical Technology, The Hong Kong Polytechnic University, Hung Hom, Hong Kong, P. R. China. E-mail: wai-yeung.wong@polyu.edu.hk

† Electronic Supplementary Information (ESI) available: [Synthetic details, UV-visible spectra and cell imaging data]. See DOI: 10.1039/x0xx00000x

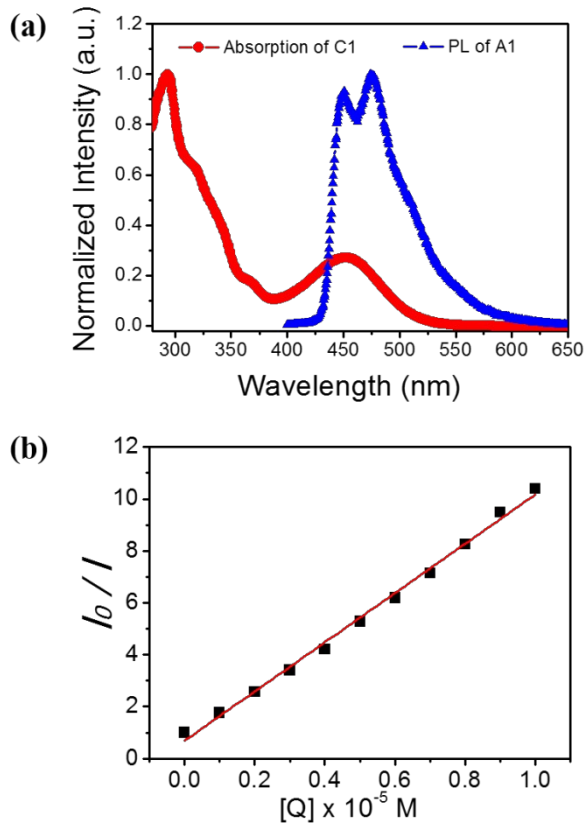

Fig. 1 (a) Normalized absorption and photoluminescence spectra of **A1** and **C1** in CH_3CN solution. (b) Stern-Volmer plot of the quenching study between **A1** and **C1** ([Q] is the concentration of quencher). The final concentrations for **A1** and **C1** are 1 × 10^{-5} M and 3 × 10^{-5} M.

(L = 4'-phenyl-2,2':6',2''-terpyridine, L' = 3-([2,2':6',2''-terpyridin]-4'-yl)-9-hexyl-9*H*-carbazole) was selected as the cationic component. This type of iridium(III) complexes possesses a high cationic character (charge +3), which displays the following advantages: (i) three anionic iridium(III) complexes are required for the formation of a soft salt complex, and (ii) the electrostatic interactions with the anionic iridium(III) complex would be strong. These features ensure the efficient energy transfer between the two ionic complexes. Besides, the iridium(III) complex $[Ir(dfppy)_2CN_2]^-Bu_4N^+$ (**A1**) was chosen as the anionic component because its emission peak overlaps with the absorption band of **C1**. Soft salt complex **S1** was formed by these two components through electrostatic interaction. Complex **S1** exhibited enhanced $^1O_2$ generation rate and it has been successfully applied as a photosensitizer for PDT.

Results and discussion

Synthetic procedures

The soft salt **S1** complex was synthesized in two steps. Firstly, the respective anionic **A1** and cationic **C1** iridium(III) complexes were prepared. Complex **A1** was synthesized through refluxing $[Ir(dfppy)_2Cl]_2$ (dfppy = 2-(2,4-difluorophenyl)pyridine) and tetrabutylammonium cyanide (5 equiv) in dichloromethane for 5 h. The terpyridine ligands and their corresponding cationic iridium(III) complex (**C1**) were prepared according to the previous methods.[11] Then, the complex **S1** was obtained by stirring **A1** and **C1** (3 : 1 molar ratio) in the mixture of acetone-water at room temperature. The desired complexes were characterized by NMR spectroscopy, MALDI-TOF spectrometry and elemental analysis.

Photophysical properties

The photoluminescence (PL) spectrum of **A1** and absorption spectrum of **C1** were investigated in CH_3CN solution (10 μM). From Fig. 1a, it can be seen that **A1** exhibited emission peaks at 451 and 475 nm, and the absorption band of **C1** was located at around 454 nm. The emission peak of **A1** and the absorption band of **C1** are well overlapped, indicating that an efficient energy transfer might occur from **A1** to **C1**. The quenching study was carried out based on the equation of $I_0/I = 1 + k_q[Q]$, where I_0 and I refer to the PL intensity of **A1** with and without the quencher **C1**, k_q represents the experimental quenching rate constant and [Q] indicates the molar concentration of the quencher. Upon addition of an increasing amount of **C1** into **A1** a CH_3CN solution (3 × 10^{-5} M), the blue emission was gradually decreased in intensity, demonstrating the

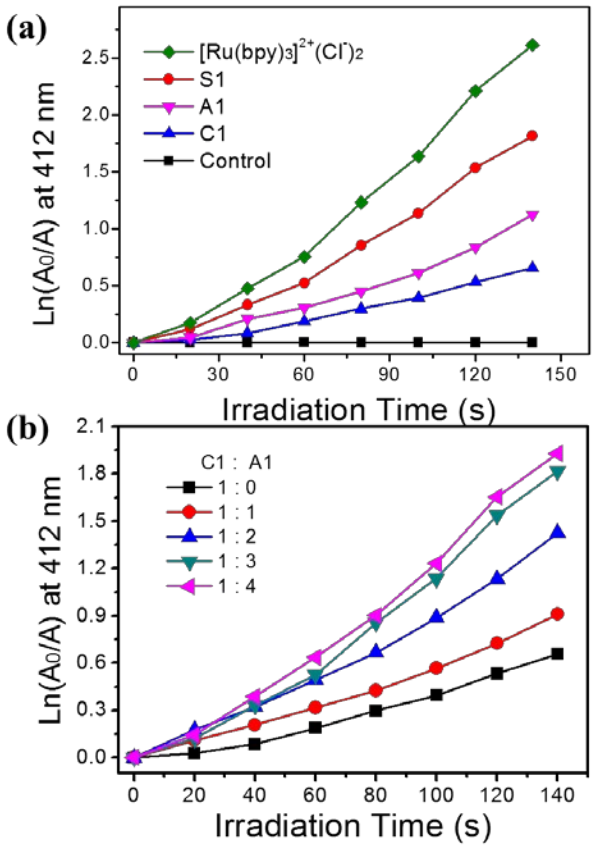

Fig. 2 (a) The decrease of DPBF absorption at 412 nm as a function of irradiation time in the presence of complexes **A1** (30 μM), **C1** (10 μM), **S1** (10 μM) and $[Ru(bpy)_3]^{2+}(Cl^-)_2$. The control plot was with only light for **S1** without DPBF. (b) The bleaching of DPBF for **C1**/**A1** versus irradiation time at a fixed equivalent of **C1** with varying **A1** equivalents. [**C1**] = 10 μM.

efficient energy transfer/quenching process between the two ionic metal complexes. The calculation of the Stern–Volmer plot of the two components yielded a k_q value of 0.94 × 10^6 M^{-1}, which suggested the superquenching behavior of **A1** by **C1**. From Fig. 1b, it indicates that the emission of **A1** and the absorption of **C1** coincide with each other and the FRET is likely to be responsible for the energy transfer in this system.

Singlet oxygen generation rate

1,3-Diphenylisobenzofuran (DPBF) was employed to detect the generation of $^1O_2$ of **A1**, **C1** and **S1**. In the presence of $^1O_2$, the absorption band of DPBF at 412 nm will decrease.[2e] As illustrated in Fig. 2a, the capability of **A1**, **C1** and **S1** to generate $^1O_2$ was measured by irradiation with a white light source (12 mW cm^{-2}). The decrease of DPBF absorption at 412 nm as a function of the irradiation time indicated that a small DPBF absorption intensity change was observed for **A1** or **C1**. In sharp contrast, the DPBF absorbance for **S1** was remarkably decreased. The DPBF bleaching rate constants (k_{obs}) in the presence of **A1**, **C1** and **S1** were measured to be 1.49 × 10^{-2} s^{-1}, 8.71 × 10^{-3} s^{-1}, and 3.68 × 10^{-2} s^{-1}, respectively. Compared with the bleaching rate for **S1**, that for **C1** was 4.23 times slower and that for **A1** was 2.46 times slower. Therefore, the generation of $^1O_2$ benefited greatly from the energy transfer between the two components. In addition, the singlet oxygen generation ability of $[Ru(bpy)_3]^{2+}(Cl^-)_2$ has been measured as the reference (Fig. 2a). Compared to the $[Ru(bpy)_3]^{2+}(Cl^-)_2$, **S1** showed lower singlet oxygen generation ability. As the energy transfer from **A1** to **C1** was dependent on their equivalent, the $^1O_2$ generation as a function of an equivalent ratio was also determined by the DPBF indicator. Fig. 2b illustrates the time curves of the decrease of absorbance of DPBF at 1.0 equivalent of **C1** with **A1** equivalent varying from 1.0 to 4.0. The bleaching rate of DPBF was observed to improve as **A1** equivalent increased, reached a peak after 3.0 equivalents (Fig. 2b). The observations mentioned above further demonstrated that the capability of $^1O_2$ generation was increased by the energy transfer from **A1** to **C1**. A possible reason is that the energy transfer between the two complexes influenced the triplet excited state generation, singlet state generation, and intersystem crossing in the whole system. In addition, the stability of **S1** in acetonitrile/buffer (1 : 9, v : v) and cell culture medium at 37 °C was investigated. Fig. S5 shows that the PL intensity at 451 nm barely changed at 37 °C even after 3 h, indicating the good stability of **S1**.

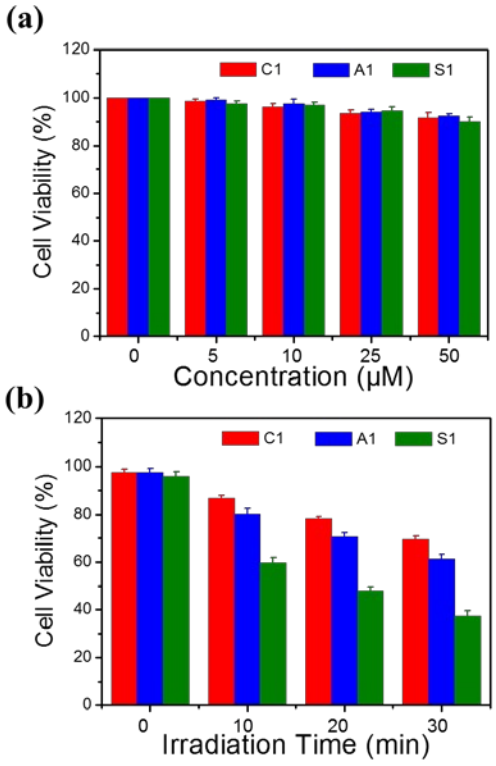

Fig. 3 In vitro cell viability of HeLa cells. (a) Cell viability values (%) assessed using an MTT test versus incubation concentrations of **A1**, **C1** and **S1** in dark. (b) The cells were incubated with **A1** (30 μM), **C1** (10 μM) and **S1** (10 μM) and then irradiated by a white light (12 mW cm^{-2}) with a xenon lamp for 10, 20 and 30 min, respectively.

PDT of cancer cells

To study the dark cytotoxicity and phototoxicity of **A1**, **C1** and **S1**, the standard methyl thiazolyl tetrazolium (MTT) assay was conducted to measure the relative viabilities of HeLa cells. Fig. 3a shows that there is no obvious cellular death after different concentrations of **A1**, **C1** and **S1** were treated to cells for 24 hours under the dark environment. The cellular viabilities were assessed to be approximately 90% even at a high concentration of 50 μM, which suggested the low cytotoxicity of these complexes in the dark. However, the cellular viabilities drastically decreased to 61%, 69% and 37% for **A1**, **C1** and **S1** (10 μM) when the cells were exposed to the white light (12 mW cm^{-2}) for 30 min. These results are consistent with the amount of $^1O_2$ generation measured in the solution. Afterwards, a systematic study was performed in order to better demonstrate the cytotoxic effect of **S1** on cancer cell viabilities.

The generation of $^1O_2$ was detected in living cells using the indicator of DCFH-DA (2',7'-dichlorofluoresceindiacetate), which can be altered to DCF (2,7-dichlorofluorescein, λ_{em} = 529 nm) with a green fluorescence in the presence of $^1O_2$. Fig. S6 shows that HeLa cells treated with DCFH-DA followed by a white light irradiation displayed very weak green fluorescence. However, intense green fluorescence was observed when **S1** was used to pre-process the cells, demonstrating the generation of intracellular $^1O_2$ as displayed in Fig. S7. In addition, the dual fluorescence of Annexin V–FITC/propidium iodide (PI) was applied to monitor the cell death caused by **S1**-mediated PDT. It can be seen from Fig. 4 that an increasing number of apoptotic cells was observed when the irradiation time was prolonged, showing that the PDT effect was enhanced by increasing the irradiation time and cytotoxicity of **S1** was low in the dark. Furthermore, flow cytometry was employed to study the PDT effect of **S1**. In flow cytometry experiments, the cell population was measured by Annexin V–$FITC^+/PI^-$ of viable cells, early apoptotic cells and necroticor late-stage apoptotic cells at various phases of cell death. In the control groups of **S1** under the dark environment and blank exposure to white light, less than 5.0% cellular death was detected (Fig. 5). In addition, the 25.8% and 18.9% cellular deaths were measured after the cells were treated by **A1** (30 μM) and **C1** (10 μM) for 24 hours and then irradiated by white

View Article Online
DOI: 10.1039/C8DT00720A

Journal Name

ARTICLE

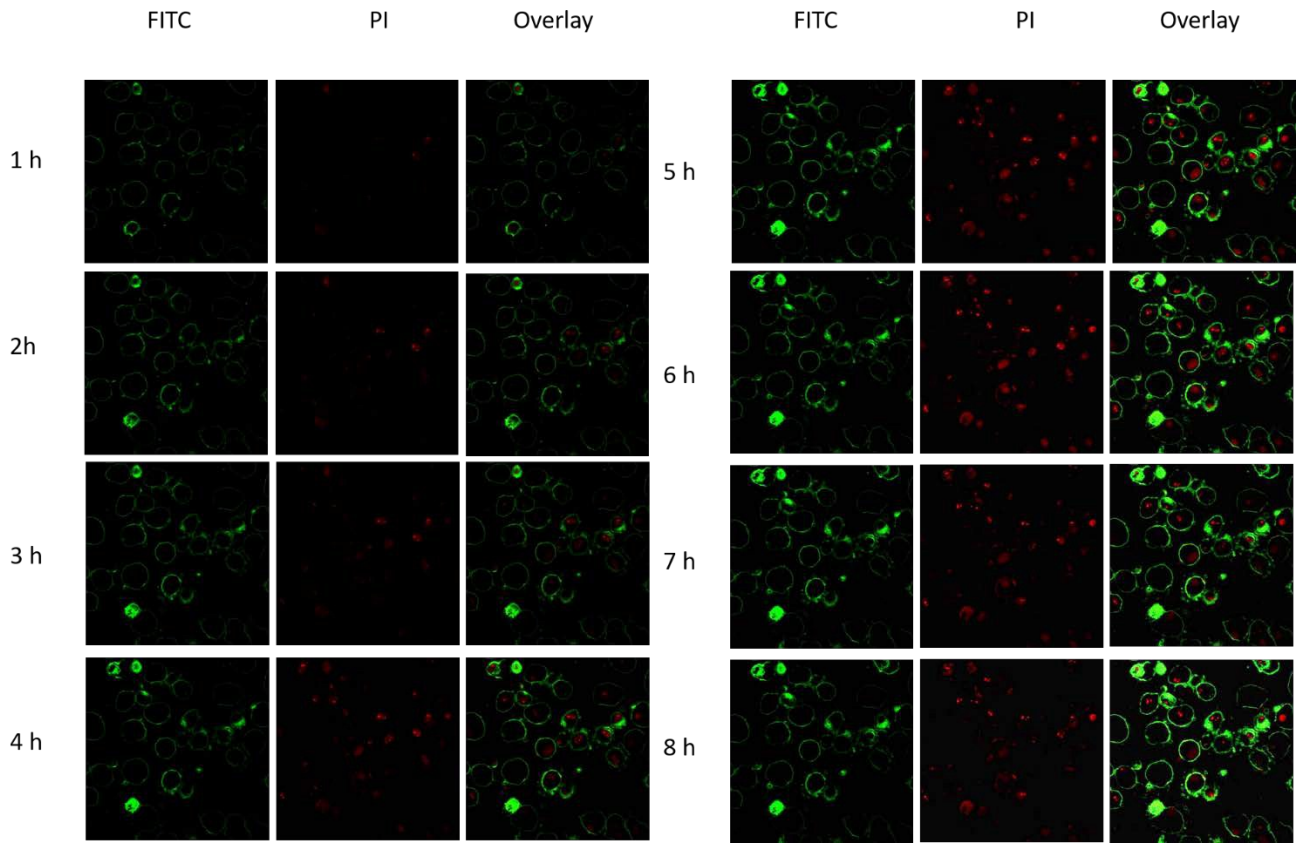

Fig. 4 Time-lapse confocal microscopy images of Annexin V–FITC/PI stained **S1** loaded Hela cells after 30 min white light irradiation (12 mW cm^{-2}).

light for 30 minutes. On the contrary, 28.3% cellular death was monitored when the cells were treated by **S1** (10 μM) for 24 hours and then irradiated by white light for 10 minutes. Prolonged irradiation time resulted in more dead cells, and 50.4% cellular death was observed when the irradiation time was 30 minutes (Fig. 5). These results indicated that **S1** could be an effective phototherapeutic candidate to cancer treatment.

Conclusions

In summary, a novel soft salt based photosensitizer, which consists of two oppositely charged ionic complexes, has been developed. The soft salt complex **S1** can generate singlet oxygen to effectively kill the cancer cells, demonstrating its potential application in PDT. Moreover, it has demonstrated that the $^1O_2$ generation rate for **S1** was 4.23-fold faster than that for **C1** and 2.46-fold faster than that for **A1**. Therefore, our design principle provides a new strategy for enhancing $^1O_2$ generation of transition-metal complexes through an efficient energy transfer from **C1** to **A1**. Our future work will focus on the development of soft salt complexes with long-wavelength absorption in order to perform *in vivo* PDT.

Experimental

Materials and methods

Commercially available chemical reagents were used without further purification. All solvents were purified before use. The solvents were carefully dried and distilled from appropriate drying agents prior to use. ^1H and ^{13}C NMR spectra were recorded with a Bruker Ultrashield 400 MHz FT-NMR spectrometer. Mass spectra were obtained with a Bruker Autoflex matrix assisted laser desorption/ionization time of flight (MALDI-TOF) mass spectrometer. UV-visible absorption spectra were recorded with a HP UV-8453 spectrophotometer. Photoluminescent spectra were measured with an Edinburgh Instrument FLS920. The irradiation during the PDT process was conducted with a xenon lamp (CEL-HXF

View Article Online
DOI: 10.1039/C8DT00720A

Journal Name

ARTICLE

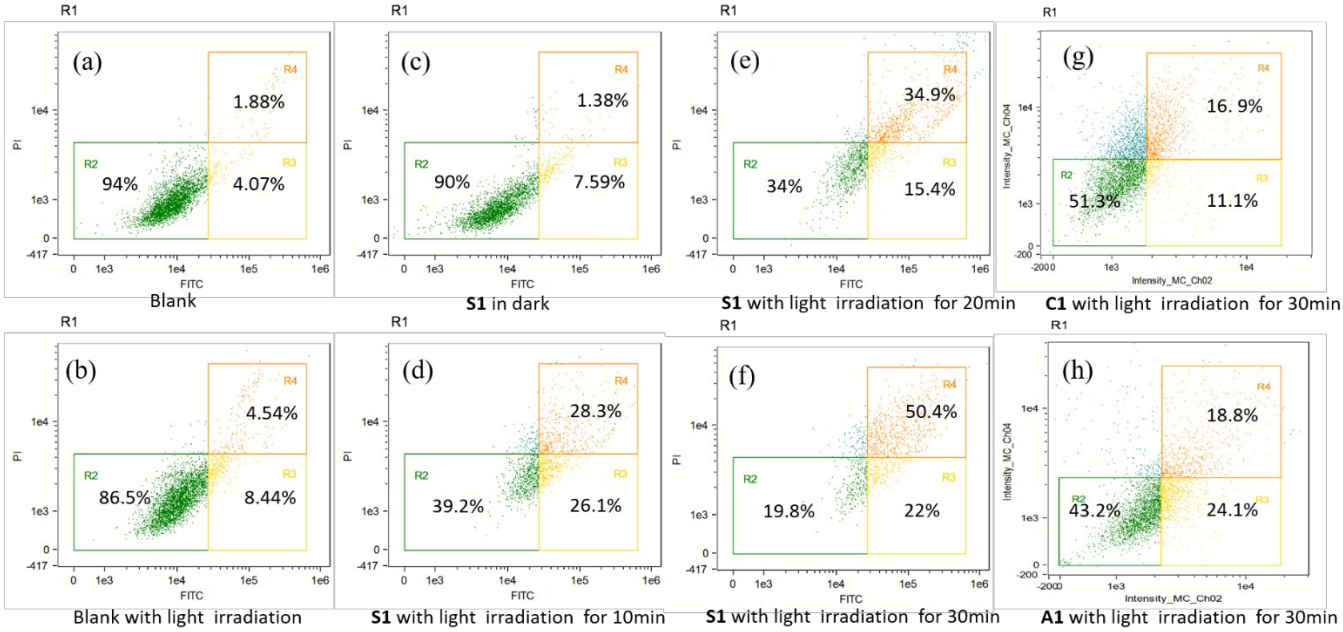

Fig. 5 Flow cytometry quantification of Annexin V–FITC/PI labeled HeLa cells under different conditions: (a) blank, (b) blank was exposed to white light (12 mW cm^{-2}) for 30 min), (c) **S1** (10 μM) under the dark and (c-f) **S1** with white light irradiation (12 mW cm^{-2}) for 10, 20 and 30 min, respectively. (g, h) **C1** and **A1** with white light irradiation (12 mW cm^{-2}) for 30 min

300, P = 300 W). Confocal luminescence imaging was carried out on an Olympus FV1000 laser scanning confocal microscope equipped with a 40 immersion objective lens. Flow cytometry experiments were conducted on FlowSight.

Synthesis and characterization

4'-Phenyl-2,2':6',2''-terpyridine. To a stirred mixture of benzaldehyde (1 mmol) and 2-acetylpyridine (4 mmol) in EtOH (10 mL), NaOH powder (4.2 mmol) and ammonia (3.0 mL) were added. After the dark pink solution had been stirred at 25 °C for 12 h, the precipitate was isolated by filtration and washed with EtOH. Purification was accomplished readily by recrystallization from ethanol. Yield 69%. ^{1}H NMR (400 MHz, $CDCl_3$) δ 8.76–8.71 (m, 4H), 8.67 (t, J = 6.4 Hz, 2H), 7.94–7.85 (m, 4H), 7.49 (dt, J = 20.0, 4.9 Hz, 3H), 7.35 (dt, J = 10.8, 5.2 Hz, 2H).

3-([2,2':6',2''-Terpyridin]-4'-yl)-9-hexyl-9*H*-carbazole. To a stirred mixture of 9-hexyl-9H-carbazole-3-carbaldehyde (1 mmol) and 2-acetylpyridine (4 mmol) in EtOH (10 mL), NaOH powder (4.2 mmol) and ammonia (3.0 mL) were added. After the dark pink solution had been stirred at 25 °C for 12 h, the precipitate was isolated by filtration and washed with EtOH. Purification was accomplished readily by recrystallization from ethanol. Yield 76%. ^{1}H NMR (400 MHz, $CDCl_3$) δ 10.10 (s, 1H), 8.62 (d, J = 1.3 Hz, 1H), 8.16 (d, J = 7.8 Hz, 1H), 8.01 (dd, J = 8.5, 1.5 Hz, 1H), 7.51 (m, 3H), 7.33 (t, J = 7.1 Hz, 1H), 4.34 (t, J = 7.3 Hz, 2H), 1.96–1.80 (m, 2H), 1.46–1.20 (m, 6H), 0.86 (t, J = 7.0 Hz, 3H).

Synthesis of C1. Firstly, the trichloroiridium(III) terpyridine complexes [Ir(ptpy)Cl_3] was synthesized from the reaction of $IrCl_3 \cdot 3H_2O$ and the ptpy ligand in degassed ethylene glycol at 160 °C for 15 min. Then, a mixture of [Ir(ptpy)Cl_3] (1 mmol) and tpyc ligand (1 mmol) in degassed ethylene glycol was heated at 180 °C for 20 min under an inert atmosphere of nitrogen in the dark. The mixture was then cooled to room temperature and a saturated aqueous solution of KPF_6 (2 mmol) was added to precipitate an orange-red solid. The solid was washed with cold water and then a mixture of methanol and ether, and then dried *in vacuo*. Subsequent recrystallisation of the complex from acetone–diethyl ether afforded C1 as air-stable orange-red crystals. Yield 46%. ^{1}H NMR (400 MHz, DMSO-d_6): δ 9.68 (s, 2H), 9.61 (s, 2H), 9.30 (s, 1H), 9.27–9.18 (m, 4H), 8.59 (d, J = 8.5 Hz, 1H), 8.44 (d, J = 7.6 Hz, 2H), 8.37 (dt, J = 14.5, 7.4 Hz, 5H), 8.05 (d, J = 8.9 Hz, 1H), 7.99 (d, J = 5.1 Hz, 2H), 7.95 (d, J = 5.3 Hz, 2H), 7.84 (t, J = 7.7 Hz, 2H), 7.76 (dd, J = 12.8, 7.9 Hz, 2H), 7.59 (dt, J = 12.6, 7.0 Hz, 5H), 7.40 (t, J = 7.6 Hz, 1H), 4.58 (t, J = 7.0 Hz, 2H), 1.94–1.74 (m, 2H), 1.50–1.17 (m, 6H), 0.82 (t, J = 7.1 Hz, 3H). ^{13}C NMR (400 MHz, DMSO-d_6): δ 158.9, 158.8,

155.5, 155.0, 154.5, 154.5, 153.7, 143.9, 142.9, 142.8, 141.4, 135.3, 132.4, 130.1, 130.0, 129.9, 128.8, 127.7, 127.6, 127.4, 126.5, 125.6, 124.0, 123.5, 123.1, 122.8, 121.5, 120.9, 120.5, 118.6, 111.0, 110.8, 31.5, 29.1, 26.6, 22.5, 14.3, 1.6. MS (MALDI-TOF): *m/z* 1274.3 (M^+). Elemental analysis (calcd, found for $C_{54}H_{45}F_{18}IrN_7P_3$): C (45.70, 45.58), H (3.20, 3.36), N (6.91, 7.14).

Synthesis of A1. 0.1 mmol Iridium(III) bis(2-(2,4-difluorophenyl)pyridine) dichloro-bridged dimer was combined with 0.1 mmol tetrabutylammonium cyanide in dichloromethane at 50 °C for 4 h. After removing dichloromethane under reduced pressure, the product was purified by column chromatography aluminum oxide with dichloromethane and methanol (10 : 1, v : v) as the eluent. Yield 73%. ^{1}H NMR (400 MHz, DMSO-d_6): δ (ppm) 9.53 (d, *J* = 8 Hz, 2H), 8.20 (d, *J* = 8 Hz, 2H), 8.02 (t, *J* = 16 Hz, 2H), 7.44 (t, *J* = 12 Hz, 2H), 6.64–6.59 (m, 12 H), 5.52 (d, *J* = 8 Hz, 2H), 3.33–3.17 (m, 8H), 1.61–1.53 (m, 8H), 1.34–1.25 (m, 8H), 0.92 (t, *J* = 16 Hz, 12H). ^{13}C NMR (100 MHz, DMSO-d_6): δ (ppm) 170.2, 163.4, 155.0, 145.8, 139.8, 137.4, 132.2, 129.6, 124.7, 123.4, 121.6, 120.1, 59.5, 31.2, 23.5, 19.7, 14.0. MS (MALDI-TOF): *m/z* 625.2 [M^-]. Elemental analysis (calcd, found for $C_{40}H_{48}F_4IrN_5$): C (55.41, 55.78), H (5.58, 5.89), N (8.08, 8.27).

Synthesis of S1. **C1** (0.1 mmol) and **A1** (0.3 mmol) were added to acetone (10 mL). The reaction mixture was stirred for 2 h at room temperature and then extracted with $CHCl_3$. Next, the solution was washed by water for several times for removing the counterions and then concentrated by rotary evaporation. The resulting solid was washed by diethyl ether to afford **S1** as a red solid. Yield 65%. ^{1}H NMR (400 MHz, DMSO-d_6) δ 9.54 (m, 4H), 9.35 (s, 2H), 9.25 (d, *J* = 4.0 Hz, 1H), 9.14 (s, 2H), 8.97 (d, *J* = 7.6 Hz, 2H), 8.78 (d, *J* = 8.0 Hz, 2H), 8.44 (d, *J* = 7.6 Hz, 1H), 8.16–8.30 (m, 14H), 7.76-7.82 (m, 17H), 7.66 (d, *J* = 7.6, 2H), 7.60 (t, *J* = 7.6, 2H), 7.47 (m, 5H), 7.28 (t, *J* = 7.2 Hz, 1H), 7.08 (t, *J* = 7.2 Hz, 4H), 6.34-6.42 (m, 6H), 5.64 (dd, *J* = 8 Hz, 3H), 4.58 (t, *J* = 7.0 Hz, 2H), 1.26–1.45 (m, 8H), 0.82 (t, *J* = 7.1 Hz, 3H). ^{13}C NMR (100 MHz, DMSO-d_6): δ 168.4, 168.3, 167.2, 158.9, 158.8, 155.5, 155.1, 154.5, 154.1, 153.8, 152.6, 152.4, 150.3, 145.3, 143.0, 142.9, 142.8, 142.6, 141.4, 139.7, 138.5, 135.2, 132.0, 130.1, 128.8, 127.8, 127.6, 127.4, 127.4, 126.5, 125.6, 124.0, 123.5, 123.2, 127.1, 122.8, 122.5, 121.6, 121.2, 121.0, 120.5, 120.3, 111.0, 110.8, 31.4, 29.0, 26.5, 22.6, 14.3, 1.6. MS (MALDI-TOF): *m/z* 1274.3 [M^+], 625.3 [M^-]. Elemental analysis (calcd, found for $C_{126}H_{81}F_{12}Ir_4N_{19}$): C (52.95, 52.78), H (2.86, 3.13), N (9.31, 9.15).

Cell culture

The cell lines Hela (human cervical cancer) were provided by the Institute of Biochemistry and Cell Biology, SIBS, CAS (China). The cells were grown in DMEM (Dulbecco's modified Eagle's medium) supplemented with 10% FBS (fetal bovine serum), 100 mg/mL streptomycin and 100 U/mL penicillin at 37 °C with 5% CO_2.

Dark cytotoxicity assay

In vitro cytotoxicity was measured by performing methyl thiazolyltetrazolium (MTT) assays on Hela cells. Cells were seeded into a 96-well cell culture plate at 104 /well, under 100% humidity, and were cultured at 37 °C with 5% CO_2 for 24 h. Different concentrations of **A1**, **C1** and **S1** (5, 10, 20, 50 and 100 μM) were then added into the wells. The cells were subsequently incubated for 24 h at 37 °C under 5% CO_2. Then, MTT (10 μL/well, 5 mg/mL) was added to each well and the plate was incubated for an additional 4 h at 37 °C under 5% CO_2. The medium was then replaced with 150 μL dimethyl sulfoxide (DMSO) per well, and OD570 was monitored by an enzyme-linked immunesorbent assay (ELISA) reader. The following formula was used to calculate the inhibition of cell growth:

Cell viability (%) = (mean of Abs. value of treatment group/mean Abs. value of control) × 100%

Cytotoxicity assay of PDT

Cells were seeded into a 96-well cell culture plate at 104 /well and allowed to adhere for 24 h. After that, the cells were incubated with **A1**, **C1** or **S1** for 22 h at 37 °C with 5% CO_2. Next, the cells were irradiated by white light (12 mW cm^{-2}) with a xenon lamp for 10, 20 and 30 min, respectively. The cell viability was measured through MTT assays.

Annexin V/ Propidium iodide (PI) assay

Hela cells were planted and allowed to adhere for 24 h. Then the cells were incubated with **S1** for 12 h at 37 °C with 5% CO_2. Then the cells were irradiated by white light (12 mW cm^{-2}) with a xenon lamp. The cell was stained with annexin V-FITC (5 μL) and PI (10 μL) at room temperature for 10 min in the dark. The fluorescence intensity of the cells was measured by confocal microscopy and flow cytometry (FlowSight) with excitation at 405 nm. Cells were viewed in green channel for annexin V (λ_{em} = 500-560 nm) and red channel for PI (λ_{em} = 600-680 nm), respectively.

Conflicts of interest

The authors declare no competing financial interest.

Acknowledgements

We are grateful for the financial support from the Hong Kong Research Grants Council (HKBU 12304715), the Hong Kong Polytechnic University (1-ZE1C), Ms Clarea Au for the Endowed Professorship (847S), the National Program for Support of Top-Notch Young Professionals, Natural Science Foundation of Jiangsu Province of China (BK20160885), the National Natural Science Foundation of China (21701087 and 21671061), Nanjing University of Posts and Telecommunications (NY216026), and Postgraduate Education Reform Project of Jiangsu Province (SJLX16-0335).

References

1 (*a*) P. R. Ogilby, *Chem. Soc. Rev.*, 2010, **39**, 3181; (*b*) K. Apel and H. Hirt, *Annu. Rev. Plant Biol.*, 2004, **55**, 373; (*c*) A. Greer,

View Article Online
DOI: 10.1039/C8DT00720A

Acc. Chem. Res., 2006, **39**, 797; (*d*) D. E. Dolmans, D. Fukumura and R. K. Jain, *Nat. Rev. Cancer*, 2003, **3**, 380.

2 (*a*) C. Schweitzer and R. Schmidt, *Chem. Rev.*, 2003, **103**, 1685; (*b*) O. Legrini, E. Oliveros and A. M. Braun, *Chem. Rev.*, 1993, **93**, 671; (*c*) A. P. Castano, P. Mroz and M. R. Hamblin, *Nat. Rev. Cancer*, 2006, **6**, 535; (*d*) K. Lu, C. He and W. Lin, *J. Am. Chem. Soc.*, 2014, **136**, 16712; (*e*) J. W. Tian, L. Ding, H. J. Xu, Z. Shen, H. X. Ju, L. Jia, L. Bao, J. S. Yu, *J. Am. Chem. Soc.*, 2013, **135**, 18850.

3 (*a*) X. Ding and B. H. Han, *Angew. Chem. Int. Ed.*, 2015, **54**, 6536; (*b*) Y. Yuan, C. J. Zhang, S. Xu and Bin Liu, *Chem. Sci.*, 2016, **7**, 1862; (*c*) H. Chen, J. Tian, W. He and Z. Guo, *J. Am. Chem. Soc.*, 2015, **137**, 1539.

4 (*a*) C. Zhu, L. Liu, Q. Yang, F. Lv and S. Wang, *Chem. Rev.*, 2012, **112**, 4687; (*b*) S. Kim, C. K. Lim, J. Na, Y. D. Lee, K. Kim, K. Choi, J. F. Leary and I. C. Kwon, *Chem. Commun.*, 2010, **46**, 1617.

5 (*a*) S. S. Lucky, K. C. Soo and Y. Zhang, *Chem. Rev.*, 2015, **115**, 1990; (*b*) P. Zhang, W. Steelant, M. Kumar and M. Scholfield, *J. Am. Chem. Soc.*, 2007, **129**, 4526; (*c*) Y. Dai, C. Xu, X. Sun and X. Chen, *Chem. Soc. Rev.*, 2017, **46**, 3830.

6 (*a*) W. Lv, Z. Zhang, K. Y. Zhang, H. Yang, S. Liu, A. Xu, S. Guo, Q. Zhao and W. Huang, *Angew. Chem. Int. Ed.*, 2016, **55**, 9947; (*b*) X. Zhou, H. Liang, P. Jiang, K. Y. Zhang, S. Liu, T. Yang, Q. Zhao, L. Yang, W. Lv, Q. Yu and W. Huang, *Adv. Sci.*, 2016, **3**, 1500155; (*c*) J. S. Nam, M. G. Kang, J. Kang, S. Y. Park, S. J. C. Lee, H. T. Kim, J. K. Seo, O. H. Kwon, M. H. Lim, H. W. Rhee and T.H. Kwon, *J. Am. Chem. Soc.*, 2016, **138**, 10968; (*d*) E. Du, X. Hu, S. Roy, P. Wang, K. Deasy, T. Mochizuki and Y. Zhang, *Chem. Commun.*, 2017, **53**, 6033.

7 (*a*) W. Y. Wong and C. L. Ho, *J. Mater. Chem.*, 2009, **19**, 4457; (*b*) H. B. Sun, S. J. Liu, W. P. Lin, K. Y. Zhang, W. Lv, X. Huang, F. W. Huo, H. R. Yang, G. Jenkins, Q. Zhao and W. Huang, *Nat. Commun.*, 2014, **5**, 3601; (*c*) Q. Zhao, L. Li, F. Li, M. Yu, Z. Liu, T. Yi and C. Huang, *Chem. Commun.*, 2008, **44**, 685; (*d*) M. S. Lowry and S. Bernhard, *Chem. Eur. J.*, 2006, **12**, 7970.

8 (*a*) C. Xing, Q. Xu, H. Tang, L. Liu and S. Wang, *J. Am. Chem. Soc.*, 2009, **131**, 13117; (*b*) T. Ishi-i, Y. Taguri, S. Kato, M. Shigeiwa, H. Gorohmaru, S. Maeda and S. Mataka, *J. Mater. Chem.*, 2007, **17**, 3341; (*c*) H. Xiong, D. Zhou, X. Zheng, Y. Qi, Y. Wang, X. Jing and Y. Huang, *Chem. Commun.*, 2017, **53**, 3422.

9 (*a*) Q. Zhao, F. Y. Li and C. H. Huang, *Chem. Soc. Rev.*, 2010, **39**, 3007; (*b*) G. J. Zhou and W. Y. Wong, *Chem. Soc. Rev.*, 2011, **40**, 2541; (*c*) K. Y. Zhang, H. Liu, M. Tang, A. W. Choi, N. Zhu, X. Wei, K. Lau and K. K. W. Lo, *Inorg. Chem.*, 2015, **54**, 6582.

10 (*a*) C. Wu, H. F. Chen, K. T. Wong and M. E. Thompson, *J. Am. Chem. Soc.*, 2009, **132**, 3133; (*b*) Y. Ma, H. Liang, Y. Zeng, H. Yang, C. L. Ho, W. Xu, Q. Zhao, W. Huang, and W. Y. Wong, *Chem. Sci.*, 2016, **7**, 3338; (*c*) S. Guo, T. Huang, S. Liu, K. Y. Zhang, H. Yang, J. Han, Q. Zhao and W. Huang, *Chem. Sci.*, 2017, **8**, 348; (*d*) M. Mauro, K. C. Schuermann, R. Prétôt, A. Hafner, P. Mercandelli, A. Sironi and L. De Cola, *Angew. Chem. Int. Ed.*, 2010, **49**, 1222; (*e*) G. Nasr, A. Guerlin, F. Dumur, L. Beouch, E. Dumas, G. Clavier, F. Miomandre, F. Goubard, D. Gigmes, D. Bertin, G. Wantze and C. R. Mayer, *Chem. Commun.*, 2011, **47**, 10698; (*f*) M. Sandroni and E. Colman, *Dalton Trans.*, 2014, **43**, 3676.

11 (*a*) W. Leslie, A. S. Batsanov, J. A. K. Howard and J. A. G. Williams, *Dalton Trans.*, 2004, 623; (*b*) D. C. Goldstein, Y. Y. Cheng, T. W. Schmidt, M. Bhadbhadec and P. Thordarson, *Dalton Trans.*, 2011, **40**, 2053.